

DFT STUDY OF THE INTERACTION BETWEEN ACETYLSALICYLIC ACID AND N, N-DIMETHYLFORMAMIDE

Abstract

The complexation of Acetylsalicylic acid and N, N-Dimethyl formamide is studied under Density Functional Theory (DFT) calculations by implementing B3LYP hybrid functional and the standard 6-31G (d,p) basis set. The intermolecular hydrogen bonds (O2-H21...O22 and C11=O3...H33) are formed between the two monomers, validated by NBO study. The nature of the interaction is characterized using AIM analysis. The reactive regions of the complex are studied by means of MEP plot. The HOMO-LUMO gap (5.59 eV) of the complex bespeaks its bioactive nature.

Keywords: DFT, NBO, MEP, HOMO-LUMO, AIM

Authors

Jyotshna Saikia

Department of Physics
NERIST,
Nirjuli, Arunachal Pradesh, India
jyotshnasaikianlp@gmail.com

Th. Gomti Devi

Department of Physics
Manipur University
Canchipur, Manipur, India.

Tado Karlo

Department of Physics
NERIST,
Nirjuli, Arunachal Pradesh, India

I. INTRODUCTION

Acetylsalicylic acid, commonly known as Aspirin, is a nonsteroidal anti-inflammatory drug (NSAID) that exhibits a broad spectrum of pharmaceutical activities including its antipyretic, analgesic, and anti-inflammatory properties. The drug shows its preventive effect against several human cancers such as breast cancer, gastric cancer and colon cancer [1]. Cancer is one of the leading causes of death around the globe. Multiple lines of evidence show that reactive oxygen species (ROS) is one of the major contributors towards the growth, progression, and regeneration of cancer cells. A high concentration of ROS level promotes metastatic tumor progression [2-4]. N,N-Dimethyl formamide (DMF), also known as Fumaric acid, is a simple aprotic polar molecule that significantly inhibited tumor metastasis by reducing reactive oxygen species (ROS) production in tumor-associated macrophages [5]. In the current article, we focus on the study of the Aspirin-DMF interaction using DFT to enlighten the reactivity of the new potent drug combination for future pharmaceutical applications.

II. COMPUTATIONAL METHODS

The computational calculations are accomplished by B3LYP/6-31G(d,p) level under DFT [6]. Gauss View 6.0 tool is used for the visualization of the geometries of the molecules. Structural optimization is carried out using Gaussian 09W software. MEP plot and HOMO-LUMO calculations are performed under the same computational level.

III. RESULTS AND DISCUSSIONS

1. Geometrical Parameters: The optimized structure of Aspirin+DMF having SCF energy 897.25 Hartree is presented in Fig.1. In Aspirin+DMF, O2-H21...O22 (1.64 Å) and C11=O3...H33 (2.31 Å) hydrogen bonds are observed to be formed between the carboxyl group of Aspirin and the carbonyl group of DMF, which leads to the structural modulation of the monomers under complexation [7]. The O2-H21, O3=C11, C6-C11, O22=C26 bonds are significantly elongated by 0.03, 0.01, 0.01, 0.01 Å, respectively, whereas, O2-C11, O1-C12 bonds are contracted by 0.02 and 0.01 Å, respectively than that of the individual states. Some of the selected bonds are displayed in Table 1.

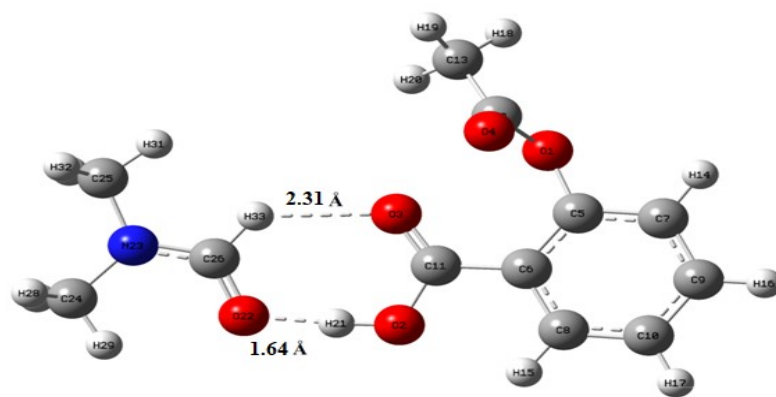


Figure 1: Optimized Structure of Aspirin+DMF.

Table 1: Optimized Bond Lengths of Aspirin, DMF, Aspirin + DMF.

Sl. No.	Aspirin		Sl. No.	DMF		Sl. No.	Aspirin + DMF	
	Bond	Bond Length (Å)		Bond	Bond Length (Å)		Bond	Bond Length (Å)
1	O1-C12	1.38	1	O1=C5	1.22	1	O1-C12	1.37
2	O1-C5	1.38	2	N2-C5	1.36	2	O1-C5	1.38
3	O2-H21	0.97	3	N2-C3	1.45	3	O2-H21	1.00
4	O2-C11	1.35	4	N2-C4	1.45	4	O2-C11	1.33
5	O3=C11	1.21	5	C3-H6	1.09	5	O3=C11	1.22
6	O4=C12	1.20	6	C3-H7	1.09	6	O4=C12	1.20
7	C5-C6	1.40	7	C3-H8	1.09	7	C5-C6	1.40
8	C5-C7	1.39	8	C4-H9	1.09	8	O22=C26	1.23
9	C6-C8	1.40	9	C4-H10	1.09	9	N23-C26	1.35
10	C6-C11	1.48	10	C4-H11	1.09	10	C25-H32	1.09
11	C7-C9	1.39	11	C5-H12	1.10	11	C26-H33	1.09

- 2. Natural Bond Orbital (NBO) Analysis:** The intermolecular hydrogen bond formation between Aspirin and DMF is confirmed by NBO study that demonstrates the electron density transfer from $n_2(O22) \rightarrow \sigma^*(O2-H21)$ and $n_2(O3) \rightarrow \sigma^*(C22-H33)$ orbital leading stabilization of the system with energy values ($E^{(2)}$) of 15.93 kcal/mol and 0.45 kcal/mol, respectively. The highest stabilization of energy 114.46 kcal/mol is obtained due to the interaction between the donor orbital $\pi^*(C5-C6)$ and the acceptor orbital $\pi^*(O3-C11)$. Selected donor-acceptor interactions are portrayed in Table 2.

Table 2: Some Selected Interactions Between Donor (Lewis-Type) and Acceptor (Non-Lewis) Orbitals of Aspirin+DMF.

Donor (i)	Acceptor (j)	$E^{(2)}$ (kcal/mol)	$E(j) - E(i)$ (a.u.)	F_{ij} (a.u.)
Within unit 1				
$\sigma(O2-H21)$	$\sigma^*(C6-C11)$	4.48	1.19	0.066
$\pi(C5-C6)$	$\pi^*(O3-C11)$	10.94	0.30	0.052
$\pi(C5-C6)$	$\pi^*(C7-C9)$	17.95	0.29	0.065
$\pi(C5-C6)$	$\pi^*(C8-C10)$	20.63	0.29	0.070
$\pi(C7-C9)$	$\pi^*(C5-C6)$	22.01	0.28	0.071
$\pi(C7-C9)$	$\pi^*(C8-C10)$	19.02	0.29	0.066
$\pi(C8-C10)$	$\pi^*(C7-C9)$	21.41	0.28	0.070
$n_2(O1)$	$\pi^*(O4-C12)$	41.30	0.34	0.106
$n_2(O2)$	$\pi^*(O3-C11)$	47.62	0.34	0.114
$n_2(O3)$	$\sigma^*(O2-C11)$	29.02	0.65	0.124
$n_2(O3)$	$\sigma^*(C6-C11)$	19.61	0.68	0.105
$n_2(O4)$	$\sigma^*(O1-C12)$	37.52	0.59	0.134
$n_2(O4)$	$\sigma^*(C12-C13)$	18.45	0.64	0.100
$\pi^*(C5-C6)$	$\pi^*(O3-C11)$	114.46	0.01	0.058

From 1 to 2				
$n_2(O3)$	$\sigma^*(C26-H23)$	0.63	0.67	0.019
$n_1(O3)$	$\sigma^*(C26-H33)$	0.45	1.09	0.020
From 2 to 1				
$n_2(O22)$	$\sigma^*(O2-H21)$	15.93	0.78	0.102
Within unit 2				
$n_2(O22)$	$\sigma^*(N23-C26)$	24.55	0.69	0.118
$n_2(O22)$	$\sigma^*(C26-H33)$	14.20	0.71	0.092
$n_1(N23)$	$\sigma^*(O22-C26)$	20.17	0.48	0.091
$\sigma(O22-C26)$	$\pi^*(O22-C26)$	74.22	0.18	0.283

3. Molecular Electrostatic Potential (MEP) Analysis:

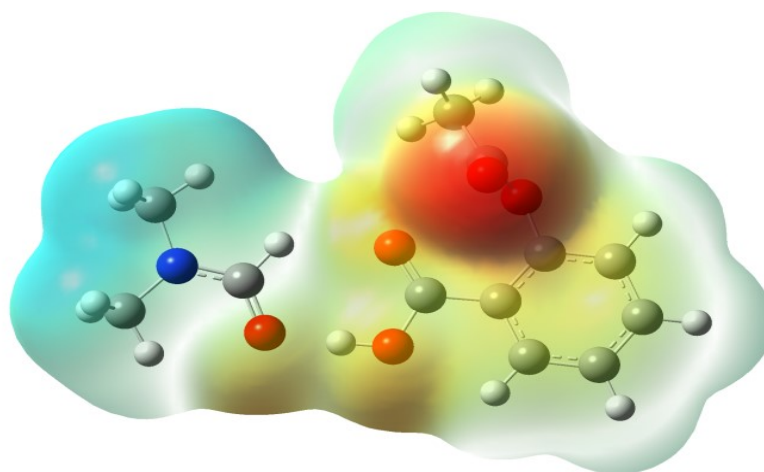


Figure 2: MEP Surface of Aspirin + DMF.

MEP surface of Aspirin+DMF generated using DFT is portrayed in Fig. 2. The existence of both electropositive and electronegative potential areas indicated by blue and red colour, respectively demonstrates the electron donating and accepting tendency, thereby bespeaks the reactive nature of the complex [8]. The blue regions are found covering the hydrogen atoms attached with nitrogen atoms and red regions are noticed over the oxygen atoms.

- 4. Frontier Molecular Orbitals (FMOs) Analysis:** FMO energy gap is an important descriptor to predict the bioactivity of a complex. The combination of the highest occupied and lowest unoccupied molecular orbitals (HOMO and LUMO) is termed as FMOs are generally used for the computation of several quantum chemical parameters that describe the stability as well as reactivity of the molecule. The HOMO and LUMO orbitals of Aspirin + DMF are shown in Fig. 3. $E_{LUMO} - E_{HOMO}$ is found as 5.59 eV and the hardness is computed as 2.79 eV, which is comparable to the reported bioactive molecules [9, 10]. Table 3 shows the calculated quantum chemical parameters of Aspirin + DMF.

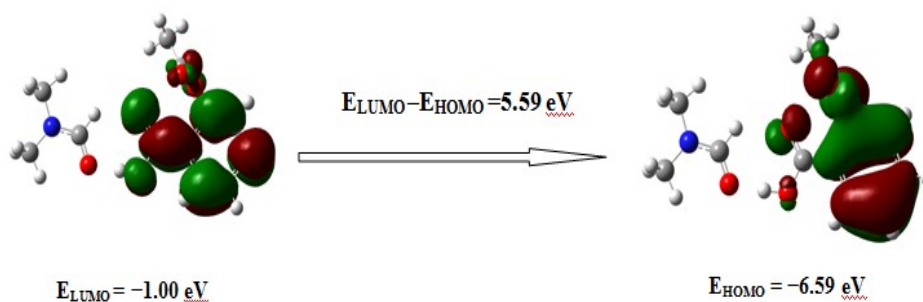


Figure 3: FMOs of Aspirin + DMF.

Table 3: Quantum Chemical Parameters of Aspirin + DMF.

Parameters	Aspirin + DMF
E_{LUMO} (eV)	- 1.00
E_{HOMO} (eV)	- 6.59
$E_{LUMO} - E_{HOMO}$ (eV)	5.59
Hardness (η) (eV) $= 1/2(E_{LUMO} - E_{HOMO})$	2.79
Chemical potential (μ) (eV) $= 1/2(E_{HOMO} + E_{LUMO})$	3.79
IE (eV) = $-E_{HOMO}$	6.59
EA (eV) = $-E_{LUMO}$	1.00
Global electrophilicity index (ω) = $\mu^2/2\eta$	2.57

- 5. AIM Analysis:** Quantum theory of atoms in molecules (AIM) as proposed by Bader's suggests a way to analyze the strength as well as the nature of hydrogen bonds at the bond critical points in molecules in terms of topological parameters like electron density (ρ) and its laplacian values ($\nabla^2 \rho$), energy density ($H(r)$), potential energy density $V(r)$ and Lagrangian K.E. $G(r)$. Hydrogen bonds are categorized as (i) strong and covalent if $\nabla^2 \rho_{BCP} < 0$ and $H_{BCP} < 0$, (ii) medium with partially covalent if $\nabla^2 \rho_{BCP} > 0$ and $H_{BCP} < 0$, and (iii) weak with electrostatic nature if $\nabla^2 \rho_{BCP} > 0$ and $H_{BCP} > 0$ [11-12]. AIM molecular graph of Aspirin+DMF generated using the AIM theory and B3LYP/6-31 G(d,p) methodology by Multiwfn software is depicted in Fig. 4. Table 4 portrays that O2-H21...O22-C26 hydrogen bond has $H(r)$ value as -0.0021 and $\nabla^2 \rho$ values as 0.1402 indicating its partially covalent nature with its medium strength. C11-O3...O1-C5 and C11-O3...H33-C26 have positive values for both $H(r)$ and $\nabla^2 \rho$ referring their weak nature with electrostatic characteristics. The energy of the O2-H21...O22-C26 hydrogen bond is measured as 12.33 kcal/mol , which is found greater as compared to the other H-bonds.

Table 4: Topological Parameters at the Bond Critical Points of Aspirin + DMF

Hydrogen bonds	ρ_{BCPs}	$\nabla^2 \rho_{\text{BCPs}}$	H(r)	G(r)	V(r)	E_{bond} (kcal/mol)
C11–O3···O1–C5	0.0149	0.0547	0.0007	0.0129	–0.0122	3.82
O2–H21···O22–C26	0.0511	0.1402	–0.0021	0.0371	–0.0393	12.33
C11–O3···H33–C26	0.0143	0.0433	0.0003	0.0105	–0.0101	3.16

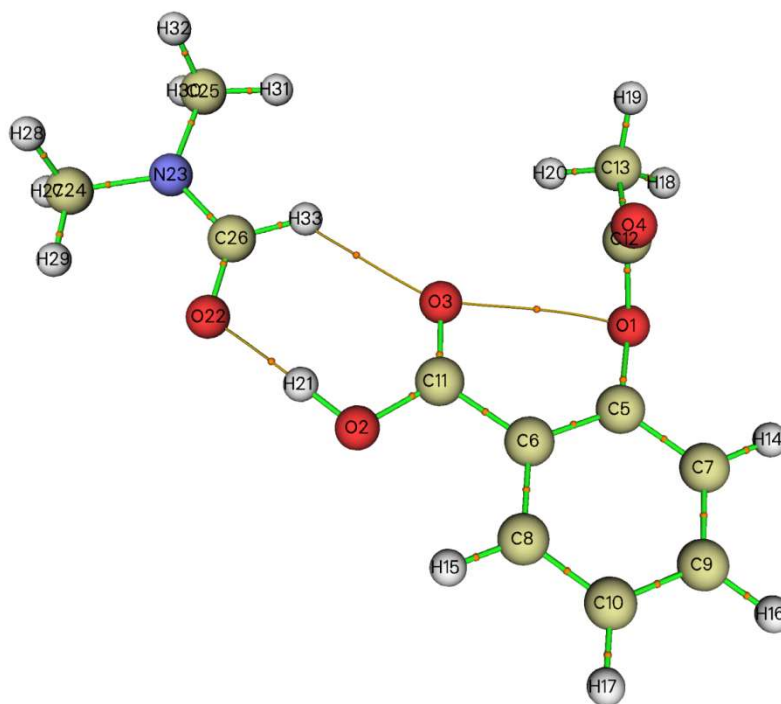


Figure 4: AIM Graph of Aspirin + DMF.

IV. CONCLUSION

Geometrical optimization of Aspirin+DMF is done using DFT-B3LYP/6-31G(d,p) calculations that shows the presence of O2–H21···O22 (1.64 Å) and C11=O3···H33 (2.31 Å) hydrogen bonds in the complex, which is further confirmed by NBO analysis. The stabilization energy associated with O2–H21···O22 bond is higher as compared to the C11=O3···H33 bond indicating the more intense interaction. AIM results further demonstrate that O2–H21···O22–C26 bond is stronger with partially covalent nature. MEP plot shows the reactive areas in the complex. The FMO gap of the complex is calculated as 5.59 eV representing its bioactive nature.

V. ACKNOWLEDGEMENT

The author (J. Saikia) gratefully acknowledges the funding by Department of Science and Technology (DST), by way of Inspire fellowship (Grant No. DST/INSPIRE Fellowship/2019/IF190217) during the research work.

REFERENCES

- [1] J. Liu, F. Zheng, M. Yang, X. Wu, and A. Liu, *Medicine (Baltimore)*, Vol. 100(33), pp. e26870, 2021.
- [2] V. Aggarwal, H.S. Tuli, A. Varol, F. Thakral, M.B. Yerer, K. Sak, M. Varol, A. Jain, M.A. Khan, and G. Sethi, *Biomolecules*, vol. 9(11), pp. 735, 2019.
- [3] G.Y. Liou, and P. Storz, *Free Radic Res.* Vol. 44(5), pp. 479-96, 2010.
- [4] B. Perillo, M. Di Donato, and A. Pezone, *Exp Mol Med*, vol. 52, pp. 192–203, 2020.
- [5] Y. Li, Y. Jia, Y. Xu, and K. Li, *Front. Oncol.* Vol. 11, pp. 706448, 2021.
- [6] J. Saikia, B. Borah, and T.G. Devi, *J. Mol. Struct.* Vol. 1227, pp.129664, 2021.
- [7] J. Saikia, T.G. Devi, and T. Karlo, *J. Mol. Struct.* Vol. 1250, pp. 131889, 2022.
- [8] M.M. Borah, and T.G. Devi, *J. Mol. Struct.* Vol. 1136, pp. 182–195, 2017.
- [9] B. Borah, and T.G. Devi, *J. Mol. Struct.* Vol. 1221, pp. 128819, 2020.
- [10] Saral, P. Sudha, S. Muthu, and A. Irfan, *J. Mol. Struct.* Vol. 1247, pp. 131414, 2022.
- [11] Rozas, I. Alkorta, and J. Elguero, *J. Am. Chem. Soc.* Vol. 122, pp. 11154–11161, 2000.
- [12] J. Saikia, T.G. Devi, and T. Karlo, *J. Mol. Struct.* Vol. 1286, pp. 135546, 2023.